Periselective Intramolecular Cycloaddition of Allene-1,3-dicarboxylates. Unusual Structural Feature of [2 + 2] Cycloadducts

Mitsutaka Yoshida,[1a] Yukari Hidaka,[1a] Yoshiharu Nawata,[1b] Jerzy M. Rudziński,[1c,d] Eiji Ōsawa,*[1c] and Ken Kanematsu*[1a]

Contribution from the Institute of Synthetic Organic Chemistry, Faculty of Pharmaceutical Sciences, Kyushu University, Fukuoka 812, Japan, Drug Development Laboratories, Chugai Pharmaceutical Company, Ltd., Tokyo 171, Japan, and Department of Chemistry, Faculty of Science, Hokkaido University, Sapporo 060, Japan. *Received July 20, 1987*

Abstract: Low-LUMO esters (**5a–d**) of 1-(methoxycarbonyl)allene-3-carboxylic acid with derivatives of 2-cyclohexen-1-ol (**2a–d**) have been prepared and their intramolecular cycloadditions studied. When there was no steric congestion in the transition state, the reaction gave [4 + 2] cycloadducts in high yields. When substituents were introduced strategically into the alcohol part of allenic ester in such a way that the [4 + 2] transition state would be sterically congested, novel [2 + 2] cycloadducts were obtained in 30–40% yields. The structures of [2 + 2] adducts were confirmed by single-crystal X-ray analyses to be strained tricyclic systems containing a cyclobutane ring fused angularly to a *cis*-hexahydrocoumarin skeleton (**6c,d**). These molecules contained an abnormally long C–C bond at different sites of the cyclobutane ring. Molecular mechanics calculations indicate that the bond elongation is caused by the through-bond π/σ^* orbital interaction and that the observed site differentiation in the orbital interaction is caused by internal steric interaction among substituents.

Previously, we have demonstrated switching of reaction pathway in the intramolecular cycloaddition of allenecarboxylates: the choice between [4 + 2] and [2 + 2] intramolecular cycloaddition depends on a conformational feature in the presumed transition-state structure.[2]

As part of our research program on the intramolecular cycloaddition reaction, we report here periselective cycloaddition of allene-1,3-dicarboxylates, which were expected to have higher reactivity than allenecarboxylates according to the results of AM1 calculations. The intramolecular cycloaddition of allene-1,3-dicarboxylates **5c** and **5d** proceeded stereoselectively to afford highly strained [2 + 2] cycloadducts **6c** and **6d**. Surprisingly, **6c** was obtained enantioselectively.

Theoretical Expectation. Effects of substituents on the HOMO/LUMO energy levels of allene (**1**) are studied by AM1 calculations. Electron-releasing methoxy (**1b**) mainly increases one of the degenerate HOMO levels, whereas electron-withdrawing cyano (**1c**) and methoxycarbonyl (**1d**) decrease LUMO to negative levels. 1,3-Bis(methoxycarbonyl) (**1e,f**) is the most effective in decreasing LUMO (Table I; Figure 1).[3]

Results

Esterification of readily available derivatives of 2-cyclohexen-1-ol **2** with half-ester **3**[4] derived from diethyl 1,3-acetonedicarboxylate followed by dehydrochlorination gave allene-1,3-dicarboxylates **5** in high yields (Scheme I).

Intramolecular Cycloaddition. Heating of allene-1,3-dicarboxylates (**5a,b**) in *o*-xylene for 2 h at 145 °C gave the corresponding [4 + 2] cycloadducts, **6a** (yield 95%) and **6b** (69%), as epimeric mixtures (**6a**, 10:3; **6b**, 6:1; Scheme II). Since the mixtures could not be separated by column chromatography on silica gel, these were aromatized into **7a** and **7b** by further thermal treatments accelerated by addition of 5% Pd–C. Structures of these compounds are assigned by inspection of spectra, as summarized in Table II. Mass spectra of these adducts clearly showed molecular ion peaks. IR spectra of **6a** and **6b** exhibited a band characteristic to δ-lactone at 1705 cm^{-1}, while their ^1H NMR spectra showed two olefinic proton signals. ^1H NMR spectra of **7a** and **7b** showed the AB pattern of aromatic protons. These assignments were fully confirmed by spin-decoupling experiments.

Table I. AM1 HOMO/LUMO Energies and Heats of Formation of Allene Derivatives (**1a–f**)

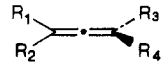

1	R_1	R_2	R_3	R_4	heat of formation, kcal/mol	HOMO, eV	LUMO, eV
a	H	H	H	H	46.14	−10.14	1.24
b	CH_3O	H	H	H	5.18	−9.24	1.08
c	CN	H	H	H	76.12	−10.44	−0.01
d	X[a]	H	H	H	−38.57	−10.62	−0.07
e, f	X	H	X[b]	H[b]	−120.90	−11.00	−0.52

[a] X = COOMe. [b] R_3 or R_4.

Scheme I

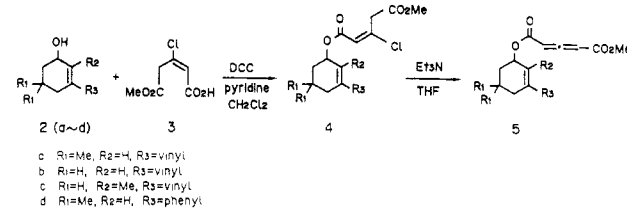

Scheme II

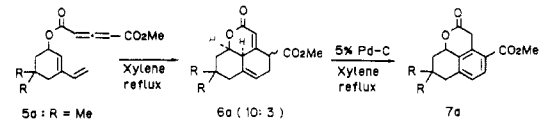

Scheme III

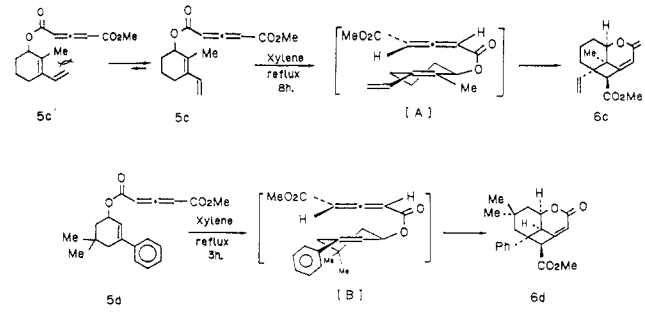

(1) (a) Kyushu University. (b) Chugai Pharmaceutical Co., Ltd. (c) Hokkaido University. (d) Permanent address: Institute of Chemistry, Wroclaw University, 50-383 Wrocaw, F. Joliot-Curie 14, Poland.

(2) (a) Yoshida, M.; Hiromatsu, M.; Kanematsu, K. *Heterocycles* **1986**, *24*, 881. (b) Yoshida, M.; Hiromatsu, M.; Kanematsu, K. *J. Chem. Soc., Chem. Commun.* **1986**, 1168.

(3) MNDO gave essentially the same results.

(4) Dell, C. P.; Smith, E. H. *J. Chem. Soc., Perkin Trans. 1* **1985**, 747.

0002-7863/88/1510-1232$01.50/0

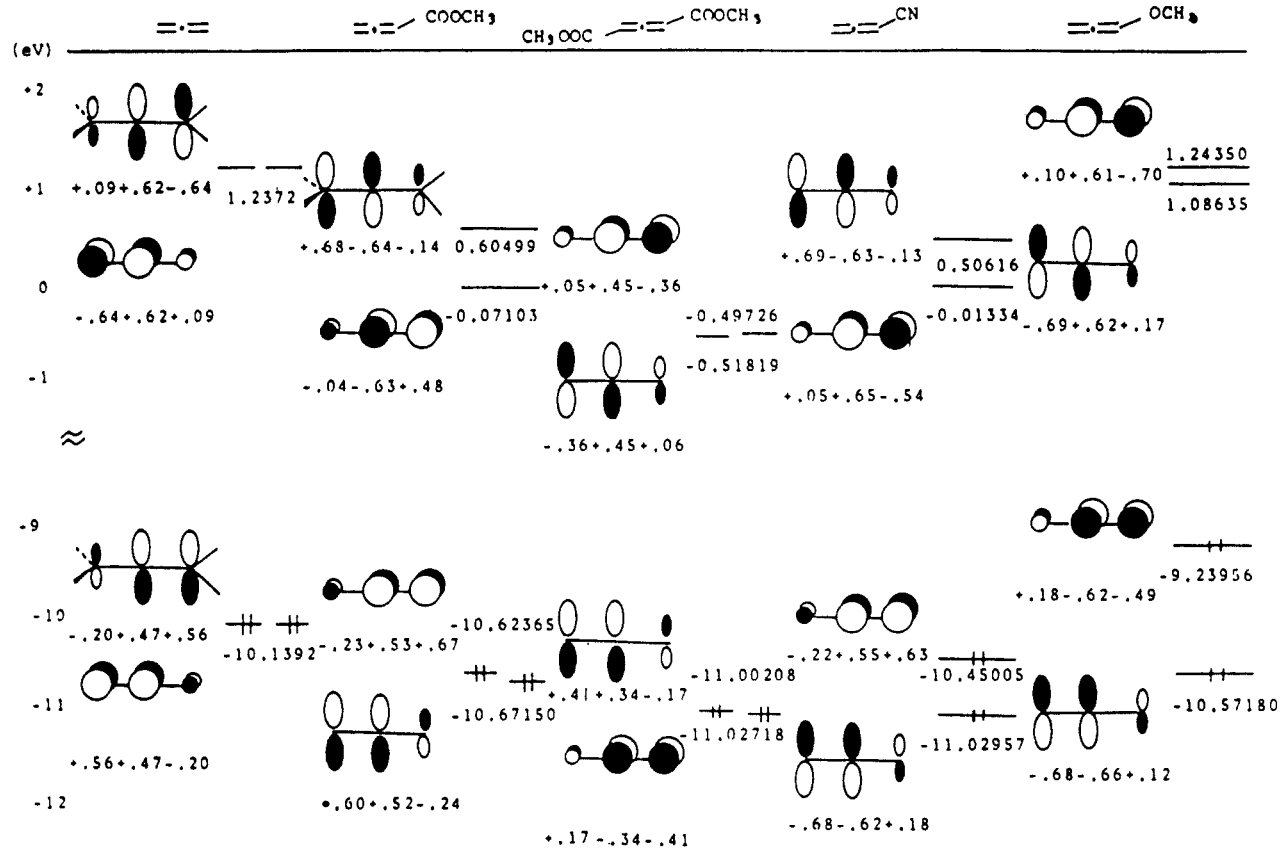

Figure 1. AM1 FMO energy levels and coefficients of **1**.

Table II. Yield and Spectral Data for Adducts

adduct	yield,[a] %	mp, °C	IR (δ-lactone),[b] cm^{-1}	^1H NMR,[c] δ (*J*, Hz)	MS, *m/z*
6a	95	oil	1705	0.90 (s, 3 H), 0.99 (s, 3 H), 1.56–2.17 (m, 4 H), 2.56–2.88 (m, 2 H), 3.10–3.60 (m, 2 H), 3.78 (s, 3 H), 4.78 (m, 1 H), 5.40 (m, 1 H), 5.93 (dd, 1 H, *J* = 1.82, 1.65)	276 (M^+)
6b	69	156	1705	3.75 (s, 3 H), 5.44 (m, 1 H), 5.84 (dd, 1 H, *J* = 1.65, 1.32)[d] 1.59–2.71 (m, 8 H), 3.04 (m, 1 H), 3.59 (dd, 1 H, *J* = 8.5, 8.8), 3.79 (s, 3 H), 4.68 (m, 1 H), 5.37 (m, 1 H), 5.85 (t, 1 H, *J* = 1.2)	248 (M^+)
7a	79	153–154	1710	3.76 (s, 3 H), 5.92 (d, 1 H, *J* = 1.2)[d] 1.0 (s, 3 H), 1.16 (s, 3 H), 1.72–2.71 (m, 4 H), 3.65 (d, 1 H, *J* = 18), 3.91 (s, 3 H), 4.86 (d, 1 H, *J* = 18), 5.35 (dd, 1 H, *J* = 7.0, 11.0), 7.12 (d, 1 H, *J* = 8), 7.88 (d, 1 H, *J* = 8.0)	274 (M^+)
7b	35[e]	181–182	1715	1.76–2.92 (m, 6 H), 3.60 (d, 1 H, *J* = 18.8), 3.91 (s, 3 H), 4.86 (d, 1 H, *J* = 18.8), 5.34 (m, 1 H), 7.14 (dd, 1 H, *J* = 0.7, 8.1), 7.87 (d, 1 H, *J* = 8.1)	246 (M^+)
6c	32	158–160	1705	1.32 (s, 3 H), 1.18–2.38 (m, 6 H), 3.79 (s, 3 H), 4.28 (m, 2 H), 5.28 (dd, 1 H, *J* = 0.7, 10.7), 5.30 (d, 1 H, *J* = 17), 5.99 (dd, 1 H, *J* = 10.7, 17.1), 6.16 (d, 1 H, *J* = 2.3)	262 (M^+)
6d	41	195–197	1715	0.55 (s, 3 H), 0.91 (s, 3 H), 1.53–2.13 (m, 5 H), 3.87 (s, 3 H), 3.97 (d, 1 H, *J* = 2.4), 5.03 (m, 1 H), 6.18 (dd, 1 H, *J* = 2.4, 2.7), 7.5 (m, 5 H)	326 (M^+)

[a] Isolated yields unless otherwise noted. [b] $CHCl_3$. [c] $CDCl_3$. [d] Chemical shifts of distinct protons from minor epimer. [e] Quantitative yield upon recovery of unreacted **6b**.

Thus, it is clear that **5a** and **5b** gave [4 + 2] adducts.

In contrast, heating of **5c** and **5d** afforded crystalline [2 + 2] cycloadducts **6c** (32%) and **6d** (41%), respectively (Scheme III).

Structures of **6c** and **6d** were first deduced from the spectroscopic data in Table II. Mass spectra of these compounds clearly showed molecular ion peaks, and the δ-lactone band appeared at 1710 cm^{-1}. ^1H NMR spectra indicated the presence of an olefinic proton in addition to vinyl (**6c**) or phenyl (**6d**) protons. These data are compatible with the [2 + 2] structure of *cis*-hexahydrocoumarin[5] with a methylene bridge.[6]

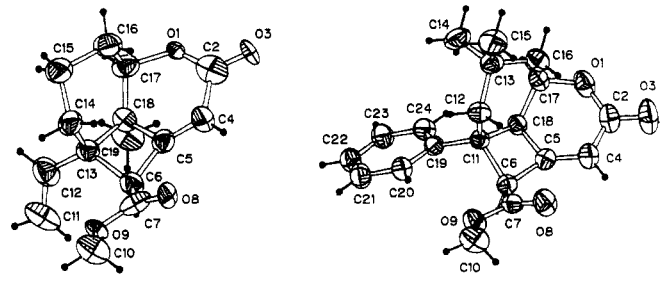

(6c) (6d)

Figure 2. ORTEP drawing of X-ray determined structures of **6c** and **d**.

Unequivocal support for the proposed structure was obtained by single-crystal X-ray analyses (Figure 2). The final atomic

(5) *cis*-4a,5,6,7,8,8a-Hexahydrocoumarin:

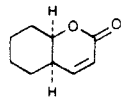

Table III. Fractional Coordinates (Esd) of **6c**

atom	x	y	z	B,[a] Å²
O1	0.1017 (1)	0.7023 (3)	0.5836 (2)	4.44 (4)
C2	0.1949 (2)	0.7960 (4)	0.6529 (3)	4.38 (6)
O3	0.1923 (2)	0.9092 (3)	0.7672 (3)	6.16 (5)
C4	0.2938 (2)	0.7501 (4)	0.5895 (3)	4.07 (5)
C5	0.2936 (2)	0.5987 (3)	0.5021 (3)	3.19 (4)
C6	0.3568 (2)	0.5021 (3)	0.3845 (3)	3.20 (4)
C7	0.4324 (2)	0.5982 (4)	0.2915 (3)	3.58 (5)
O8	0.4661 (2)	0.7446 (3)	0.3301 (3)	5.63 (4)
O9	0.463 (1)	0.5022 (3)	0.1569 (2)	4.82 (4)
C10	0.5254 (2)	0.5822 (5)	0.0483 (4)	5.63 (7)
C11	0.3023 (2)	0.1277 (4)	0.2284 (5)	6.04 (7)
C12	0.2297 (2)	0.2522 (4)	0.1948 (4)	4.69 (6)
C13	0.2417 (2)	0.4382 (3)	0.2609 (3)	3.24 (4)
C14	0.1979 (2)	0.5635 (4)	0.0950 (3)	3.83 (5)
C15	0.0760 (2)	0.6052 (5)	0.0680 (3)	4.72 (6)
C16	0.0620 (2)	0.7076 (4)	0.2394 (3)	~4.73 (6)
C17	0.0907 (2)	0.593	0.4140 (3)	3.92 (5)
C18	0.1945 (2)	0.4841 (3)	0.4381 (3)	3.24 (4)
C19	0.1944 (2)	0.3279 (4)	0.5688 (4)	4.89 (6)
H4	0.352 (2)	0.826 (4)	0.615 (3)	
H6	0.392 (2)	0.411 (4)	0.444 (3)	
H10	0.534 (2)	0.509 (4)	−0.042 (3)	
H10′	0.484 (2)	0.683 (4)	−0.021 (4)	
H10″	0.597 (2)	0.621 (4)	0.127 (3)	
H11	0.277 (2)	−0.011 (4)	0.177 (3)	
H11′	0.378 (2)	0.161 (4)	0.307 (3)	
H12	0.160 (2)	0.226 (4)	0.107 (3)	
H14	0.212 (2)	0.513 (4)	−0.020 (3)	
H14′	0.239 (2)	0.674 (4)	0.112 (3)	
H15	0.033 (2)	0.484 (4)	0.061 (3)	
H15′	0.051 (2)	0.677 (4)	−0.050 (3)	
H16	−0.010 (2)	0.751 (4)	0.232 (3)	
H16′	0.107 (2)	0.820 (4)	0.261 (3)	
H17	0.027 (2)	0.506 (4)	0.417 (3)	
H19	0.266 (2)	0.268 (4)	0.598 (3)	
H19′	0.176 (2)	0.379 (4)	0.691 (3)	
H19″	0.140 (2)	0.244 (4)	0.513 (3)	

[a] Anisotropically refined atoms are given in the form of the isotropic equivalent thermal parameter defined as $^4/_3[a^2B(1,1) + b^2B(2,2) + c^2B(3,3) + ab(\cos\gamma)B(1,2) + ac(\cos\beta)B(1,3) + bc(\cos\alpha)B(2,3)]$.

coordinates are given in Tables III and IV, and structural parameters, in Tables V–VIII. A crystal of **6c** contains an unusually close contact distance of 3.33 Å between the vinyl end-carbon atom (C_{11}) and the methoxycarbonyl group (C_{10}) of a neighboring molecule (Figure 3). Several recrystallizations of **6c** gave an enantiomerically pure crystal with an ee >99% (see the Experimental Section).

Discussion

Periselectivity and Stereoselectivity. For the allene-1,3-dicarboxylate esters **5**, [4 + 2] cycloaddition gives less strained product structure than [2 + 2] cycloaddition does. Hence, when there is no steric hindrance to the [4 + 2] transition state, this reaction takes place preferentially and in good yields (**6a,b**; Table II). However, when the *s-cis*-butadiene conformation is forbidden (**5c′**; Scheme III),[7] or the styrene unit cannot preserve coplanar structure **5d**,[2b] [2 + 2] cycloaddition is enforced. These [2 + 2] cycloaddition reactions are stereoselective. This appears to have been caused by the steric interaction between the terminal methoxycarbonyl and the vinyl or phenyl groups in the transition state (Scheme III). Model manipulation suggests that the transition states [A] and [B] avoid such repulsive interaction. Thus, it appears that the most favorable mode of cyclization for the formation of the [2 + 2] cycloadducts occurs when the cyclohexene ring defines an approximate boat of half-chair conformation, and

Table IV. Fractional Coordinates (Esd) of **6d**

atom	x	y	z	B,[a] Å²
O1	0.7088 (1)	0.3865 (2)	0.5415 (1)	4.74 (4)
C2	0.7535 (2)	0.4626 (2)	0.6277 (2)	4.64 (5)
O3	0.7930 (1)	0.5537 (2)	0.5884 (2)	6.72 (5)
C4	0.7537 (1)	0.4293 (2)	0.7627 (2)	4.12 (5)
C5	0.7278 (1)	0.3083 (2)	0.7904 (2)	3.43 (4)
C6	0.7028 (1)	0.2279 (2)	0.9007 (2)	3.22 (4)
C7	0.6750 (1)	0.3040 (2)	1.0110 (2)	3.59 (4)
O8	0.6741 (1)	0.4237 (2)	1.0213 (2)	5.37 (4)
O9	0.6488 (1)	0.2197 (2)	1.0969 (1)	4.44 (3)
C10	0.6164 (2)	0.2811 (3)	1.2065 (2)	5.54 (6)
C11	0.6360 (1)	0.1578 (2)	0.8008 (2)	2.96 (4)
C12	0.5515 (1)	0.2291 (2)	0.7999 (2)	3.49 (4)
C13	0.5107 (1)	0.2668 (2)	0.6683 (2)	3.91 (5)
C14	0.4897 (2)	0.1410 (3)	0.5883 (3)	5.29 (6)
C15	0.4313 (2)	0.3445 (3)	0.6874 (3)	5.54 (6)
C16	0.5693 (2)	0.3584 (2)	0.6037 (2)	4.19 (5)
C17	0.6488 (1)	0.2880 (2)	0.5811 (2)	3.84 (5)
C18	0.6883 (1)	0.2133 (2)	0.6947 (2)	3.19 (4)
C19	0.6308 (1)	0.0060 (2)	0.8122 (2)	3.06 (4)
C20	0.6035 (1)	−0.0512 (2)	0.9204 (2)	3.90 (5)
C21	0.3012 (2)	−0.1897 (3)	0.9343 (2)	4.47 (5)
C22	0.6250 (2)	−0.2735 (2)	0.8411 (2)	4.42 (5)
C23	0.6512 (2)	−0.2180 (2)	0.7323 (2)	4.40 (5)
C24	0.6543 (1)	−0.0789 (2)	0.7182 (2)	3.69 (4)
H4	0.771 (1)	0.499 (2)	0.823 (2)	
H6	0.742 (1)	0.159 (2)	0.935 (2)	
H10	0.597 (1)	0.209 (2)	1.252 (2)	
H10′	0.658 (1)	0.338 (2)	1.247 (2)	
H10″	0.566 (1)	0.342 (2)	1.181 (2)	
H12	0.558 (1)	0.319 (2)	0.849 (2)	
H12′	0.514 (1)	0.167 (2)	0.843 (2)	
H14	0.466 (1)	0.163 (2)	0.504 (2)	
H14′	0.543 (1)	0.084 (2)	0.574 (2)	
H14″	0.454 (1)	0.082 (2)	0.630 (2)	
H15	0.392 (1)	0.289 (2)	0.728 (2)	
H15′	0.444 (1)	0.432 (2)	0.740 (2)	
H15″	0.406 (1)	0.377 (2)	0.603 (2)	
H16	0.583 (1)	0.443 (2)	0.654 (2)	
H16′	0.542 (1)	0.392 (2)	0.523 (2)	
H17	0.637 (1)	0.225 (2)	0.513 (2)	
H18	0.726 (1)	0.143 (2)	0.667 (2)	
H20	0.588 (1)	0.008 (2)	0.984 (2)	
H21	0.583 (1)	−0.225 (2)	1.006 (2)	
H22	0.625 (1)	−0.373 (2)	0.853 (2)	
H23	0.670 (1)	−0.277 (2)	0.662 (2)	
H24	0.674 (1)	−0.038 (2)	0.638 (2)	

[a] Anistropically refined atoms are given in the form of the isotropic equivalent thermal parameter defined as $^4/_3[a^2B(1,1) + b^2B(2,2) + c^2B(3,3) + ab(\cos\gamma)B(1,2) + Ac(\cos\beta)B(1,3) + bc(\cos\alpha)B(2,3)]$.

Table V. Bond Distances in Angstroms of **6c**

atom 1	atom 2	distance	atom 1	atom 2	distance
O1	C2	1.357 (3)	O9	C10	1.452 (4)
O1	C17	1.474 (3)	C11	C12	1.297 (4)
C2	O3	1.208 (3)	C12	C13	1.493 (4)
C2	C4	1.476 (4)	C13	C14	1.535 (3)
C4	C5	1.319 (4)	C13	C18	1.594 (3)
C5	C6	1.502 (3)	C14	C15	1.530 (3)
C5	C18	1.498 (3)	C15	C16	1.524 (4)
C6	C7	1.493 (3)	C16	C17	1.517 (3)
C6	C13	1.580 (3)	C17	C18	1.518 (3)
C7	O8	1.201 (3)	C18	C19	1.527 (4)
C7	O9	1.320 (3)			

[a] Numbers in parentheses are estimated standard deviations in the least significant digits.

(6) The basic skeleton of **6** is 10-oxatricyclo[5.3.1.$0^{5,11}$]undec-7(8)-en-9-one. Note that the atomic numbering used for the crystallographic results (Tables III and IV) is arbitrary. The numbering used in the Discussion conforms to the IUPAC rules (see Chart I). The unsaturated hydrocarbon analogue, 1*H*-cyclobuta[*de*]naphthalene (**8**), is known: (a) Gessner, M.; Card, P.; Shechter, H.; Christoph, G. G. *J. Am. Chem. Soc.* **1977**, *99*, 2370. (b) Bailey, R. J.; Schechter, H. *Ibid.* **1974**, *96*, 3116.

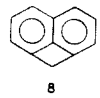

8

(7) Conformation **5c′** involves highly repulsive 1,5-interaction: Jaime, C.; Ōsawa, E. *J. Mol. Struct.* **1985**, *126*, 363.

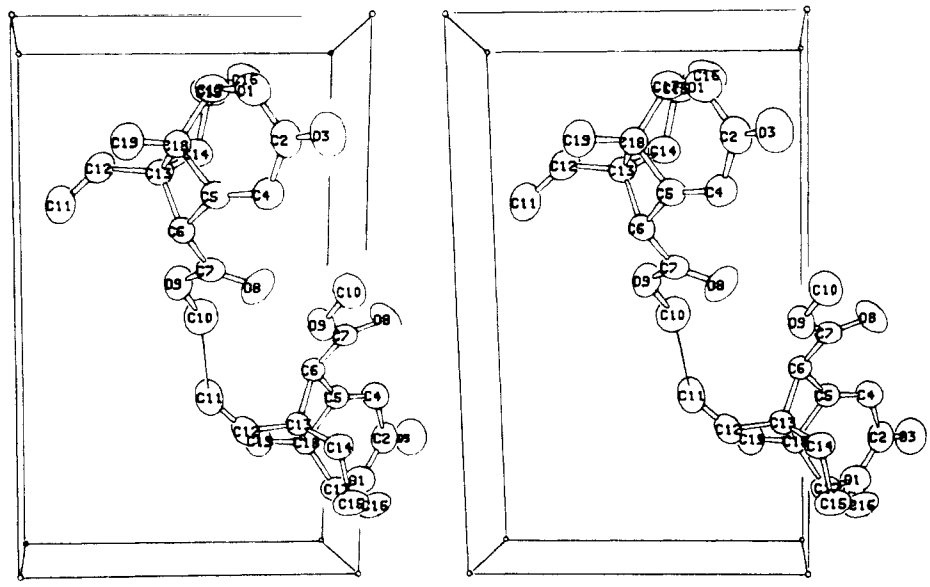

Figure 3. ORTEP stereoprojection of a unit cell of **6c**, showing close contact between the vinyl end carbon (C_{11}) and the methyl (C_{10}) of methoxycarbonyl group of a neighboring molecule.

Table VI. Bond Distances in Angstroms of **6d**[a]

atom 1	atom 2	distance	atom 1	atom 2	distance
O1	C2	1.350 (3)	C11	C19	1.519 (3)
O1	C17	1.473 (3)	C12	C13	1.538 (3)
C2	O3	1.208 (3)	C13	C14	1.535 (3)
C2	C4	1.469 (3)	C13	C15	1.538 (3)
C4	C5	1.319 (3)	C13	C16	1.528 (3)
C5	C6	1.504 (3)	C16	C17	1.512 (3)
C5	C18	1.491 (3)	C17	C18	1.510 (3)
C6	C7	1.497 (3)	C19	C20	1.389 (3)
C6	C11	1.610 (3)	C19	C24	1.388 (3)
C7	O8	1.197 (3)	C20	C21	1.388 (3)
C7	O9	1.337 (3)	C21	C22	1.376 (4)
O9	C10	1.454 (3)	C22	C23	1.382 (4)
C11	C12	1.549 (3)	C23	C24	1.395 (3)
C11	C18	1.573 (3)			

[a] Numbers in parentheses are estimated standard deviations in the least significant digits.

Chart I

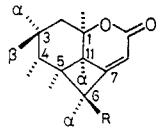

6c, 6d, 9 : R = COOMe

one possibility is through a nonsynchronous cyclization of the diradical intermediates. We suspect that **6c** formed rare conglomerate crystals,[8] since a tiny crystal selected for X-ray analysis happened to be enantiometrically pure. When recrystallization was later repeated, an enantiomer crystal was obtained (see Experimental Section).

Abnormally Long Cyclobutane Bond in 6c and 6d. The most remarkable structural feature of the [2 + 2] cycloadducts **6c** and **6d** is the presence of an unusually long C–C bond of nearly 1.6 Å in the cyclobutane ring of both of them *and in different places*: C_5–C_{11} bond (1.596 Å; note that the numbering scheme henceforth follows the IUPAC nomenclature[6] as given in Chart I) of **6c** and C_5–C_6 (1.610 Å) of **6d** are abnormally long (Table IX). MMP2 calculations[9,10] of **6c** and **6d** reproduced well the lengths of other bonds but significantly underestimated these long bonds (Table IX, italic).[11]

The abnormal elongation of these two bonds is clearly not due to steric reasons, but very likely related with the well-documented π/σ^* interaction enhanced by strain.[12] There are numerous examples where an aromatic or olefinic group destabilizes and elongates the adjacent strained C–C single bond when the π and σ^* orbitals align parallel.[12] An interesting point here is that while the substituent at C_5 should be capable of interacting with either of the cyclobutane bonds, C_5–C_6 or C_5–C_{11}, the vinyl group of **6c** seems to interact only with the latter and the phenyl group of **6d** only with the former.

A close look at the crystal conformation reveals that the π/σ^* orbitals are indeed aligned ideally with the elongated bond (Figure 4).

When **6c** is viewed along the C_5-substituent bond, the π-orbital of the vinyl group is seen almost parallel to the C_5–C_{11} bond (on the left) but nearly orthogonal to the C_5–C_6 bond (on the right). The opposite situation holds with **6d**. Clearly, the differential bond elongation is caused by the rotation of the C_5-substituent bond. Then, we ask ourselves what the reason is for the different rotation of this bond in these molecules. We find that it is the methyl group at 11α for **6c** and the one at 3α for **6d**, the carbon atoms of which are colored black in Figure 4, which determines the equilibrium rotation of the C_5-substituent bond. This is confirmed by MMP2 calculations of torsional energy curves regarding the rotation of the corresponding bond in a model structure **9** having a phenyl group at C_5 and a methyl group at various strategic positions on the same side (α) to phenyl group (Table X).

Figure 4 illustrates energy minimum conformers for each of them. It can be readily seen that the equilibrium rotation of the

(8) Jacques, J.; Collet, A.; Wilen, S. H. *Enantiomers, Racemates and Resolution*; Wiley: New York, 1981.

(9) Sprague, J. T.; Tai, J. C.; Yuh, Y.; Allinger, N. L. *J. Comput. Chem.* **1987**, *8*, 581. Standard deviation of errors in the calculation of $C(sp^3)$–$C(sp^3)$ bond distance with the MM2 scheme is 0.0093 Å. Hence, the calculated difference of 0.03 Å is significant.

(10) The following parameters are used for the α,β-unsaturated lactone function. Torsion parameters: $C(sp^2)$–$C(sp^2)$–C(=O)–O(ether), V1 = 0.34, V2 = 11.0, V3 = 0.0; $C(sp^2)$–C(=O)–O(ether)–$C(sp^3)$, V1 = 3.53, V2 = 2.3, V3 = 3.53; H–$C(sp^2)$–C(=O)–O(ether), V1 = 0.0, V2 = 16.25, V3 = 0.0; $C(sp^2)$–C(=O)–O(ether)–lone pair, V1 = V2 = V3 = 0.0, bending parameters: $C(sp^2)$–C(=O)–O(ether), k(b) = 0.7, θ(0) = 124.3. While the overall feature of structure optimized by using these parameters agrees well with the X-ray result, they are only tentative. The lactone group is located away from the cyclobutane portion, and the tentative nature of its parameters should not affect our conclusions.

(11) MMP2 relaxation of **6c** resulted in large rotation of the vinyl group, in accordance with the X-ray observation of unusually close contact in the crystal (see text).

(12) (a) Dougherty, D. A.; Choi, C. S.; Kaupp, G.; Buda, A. B.; Rudziński, J. M.; Ōsawa, E. *J. Chem. Soc., Perkin Trans. 2* **1986**, 1063. (b) Ōsawa, E.; Kanematsu, K. In *Molecular Structure and Energetics*; Greenberg, A., Liebman, J., Eds.; Verlag Chemie International: Deerfield Beach, FL, 1986; Vol. 3, Chapter 7.

Table VII. Bond Angles in Degrees of **6c**[a]

atom 1	atom 2	atom 3	angle	atom 1	atom 2	atom 3	angle
C2	O1	C17	120.3 (2)	C6	C13	C14	110.9 (2)
O1	C2	O3	117.7 (3)	C6	C13	C18	86.6 (2)
O1	C2	C4	118.4 (2)	C12	C13	C14	110.3 (2)
O3	C2	C4	123.9 (2)	C12	C13	C18	116.4 (2)
C2	C4	C5	117.4 (2)	C14	C13	C18	112.0 (2)
C4	C5	C6	140.3 (2)	C13	C14	C15	112.4 (2)
C4	C5	C18	124.2 (2)	C14	C15	C16	108.6 (2)
C6	C5	C18	93.1 (2)	C15	C16	C17	110.2 (2)
C5	C6	C7	120.7 (2)	O1	C17	C16	109.5 (1)
C5	C6	C13	86.5 (2)	O1	C17	C18	108.3 (2)
C7	C6	C13	119.2 (2)	C16	C17	C18	115.4 (2)
C6	C7	O8	125.1 (2)	C5	C18	C13	86.1 (2)
C6	C7	O9	111.0 (2)	C5	C18	C17	110.1 (2)
O8	C7	O9	123.9 (2)	C5	C18	C19	112.9 (2)
C7	O9	C10	117.1 (2)	C13	C18	C17	120.7 (2)
C11	C12	C13	128.5 (2)	C13	C18	C19	113.4 (2)
C6	C13	C12	118.8 (2)	C17	C18	C19	111.1 (2)

[a] Numbers in parentheses are estimated standard deviations in the least significant digits.

Table VIII. Bond Angles in Degrees of **6d**[a]

atom 1	atom 2	atom 3	angle	atom 1	atom 2	atom 3	angle
C2	O1	C17	120.9 (2)	C12	C13	C14	111.1 (2)
O1	C2	O3	117.4 (2)	C12	C13	C15	107.7 (2)
O1	C2	C4	119.1 (2)	C12	C13	C16	108.4 (2)
O3	C2	C4	123.4 (2)	C14	C13	C15	109.6 (2)
C2	C4	C5	116.8 (2)	C14	C13	C16	110.9 (2)
C4	C5	C6	140.7 (2)	C15	C13	C16	109.1 (2)
C4	C5	C18	123.7 (2)	C13	C16	C17	112.0 (2)
C6	C5	C18	93.5 (2)	O1	C17	C16	109.7 (2)
C5	C6	C7	117.4 (2)	O1	C17	C18	108.0 (2)
C5	C6	C11	86.2 (1)	C16	C17	C18	114.4 (2)
C7	C6	C11	120.0 (2)	C5	C18	C11	88.0 (2)
C6	C7	O8	125.6 (2)	C5	C18	C17	110.9 (2)
C6	C7	O9	110.6 (2)	C11	C18	C17	121.6 (2)
O8	C7	O9	123.8 (2)	C11	C19	C20	119.9 (2)
C7	O9	C10	116.2 (2)	C11	C19	C24	121.9 (2)
C6	C11	C12	110.7 (2)	C20	C19	C24	118.3 (2)
C6	C11	C18	86.5 (1)	C19	C20	C21	120.6 (2)
C6	C11	C19	114.8 (2)	C20	C21	C22	121.0 (2)
C12	C11	C18	112.0 (2)	C21	C22	C23	119.1 (2)
C12	C11	C19	113.6 (2)	C22	C23	C24	120.2 (2)
C18	C11	C19	116.4 (2)	C19	C24	C23	120.8 (2)
C11	C12	C13	115.4 (2)				

[a] Numbers in parentheses are estimated standard deviations in the least significant digits.

Table IX. Salient Features in the Observed and Calculated Structure of **6c** and **6d**

	bond length, Å			
	6c		**6d**	
	X-ray	MMP2	X-ray	MMP2
C_5–C_6	1.580 (3)	1.577	*1.610 (3)*	*1.585*
C_5–C_{11}	*1.596 (4)*	*1.566*	1.573 (3)	1.560
C_6–C_7	1.503 (4)	1.509	1.504 (3)	1.508
C_7–C_{11}	1.499 (4)	1.499	1.491 (3)	1.493

Table X. Substitution Patterns of **6c**, **6d**, and **9**[a]

	5α	4α	3α	3β	1α	11α	6α
6c	vinyl	H	H	H	H	Me	H
6d	Ph	H	Me	Me	H	H	H
9	Ph	H	H	H	H	H	H
4α-Me-**9**	Ph	Me	H	H	H	H	H
3α-Me-**9**	Ph	H	Me	H	H	H	H
1α-Me-**9**	Ph	H	H	H	Me	H	H
11α-Me-**9**	Ph	H	H	H	H	Me	H
6α-Me-**9**	Ph	H	H	H	H	H	Me

[a] Numbering scheme given in Chart I.

phenyl–C_5 bond changes in a counterclockwise direction from 11α-Me-**9**, 4α-Me-**9**, ..., to 3α-Me-**9**, with the phenyl group apparently avoiding steric repulsion from the methyl group. Incidentally, the observed cases of **6c** and **6d** correspond to the two extreme rotations, namely the π/σ^* orbital alignment is better in crystals than the model calculation on **9** for the vapor phase indicated. It is not clear if the better alignment in the solid state is caused by crystal packing or if it is not.

If our interpretation given above is correct, **6c** and **6d** provide the first cases of the differential elongation of strained C–C bonds through the π/σ^* interaction caused by the remote steric effect of the substituent.

Experimental Section

General Procedures. Melting points were measured with Yanagimoto micro melting point apparatus and are uncorrected. ^{1}H NMR spectra were taken with a JEOL JNM-GX 270, JEOL PS-100, or Hitachi R-600 spectrometer with tetramethylsilane as an internal standard; chemical shifts are expressed in δ values. ^{13}C NMR spectra were determined with a JEOL 100. Mass spectra were determined on a JEOL D300 equipped with a JMA 3100/3500 at an ionization voltage of 70 eV. Elemental analyses were performed on a Yanagimoto MT2 CHN recorder. For thin-layer chromatographic (TLC) analysis, Merck precoated TLC plates (Kieselgel 60 F_{254}, 0.2 mm) were used. Column chromatography was done by using Merck Kieselgel 60 (70–200 mesh) as the stationary phase.

All reactions were carried out under atmospheres of dry argon or nitrogen. All solvents were purified before use; *o*-xylene was distilled from calcium hydride.

Allene-1,3-dicarboxylates 5 were prepared in 70–90% yield from the appropriate alcohols **2** and 3-chloro-4-(methoxycarbonyl)but-2-enoic acid (**3**) according to the procedure of Dell and Smith.[4]

Methyl 3-vinyl-5,5-dimethyl-2-cyclohexenyl penta-2,3-diene-1,5-dioate (5a): pale yellow oil in 90% yield; IR (neat) 1965, 1720 cm^{-1}; ^{1}H NMR ($CDCl_3$) δ 0.97 (s, 3 H), 1.04 (s, 3 H), 1.53–2.0 (m, 4 H), 3.76 (s, 3 H),

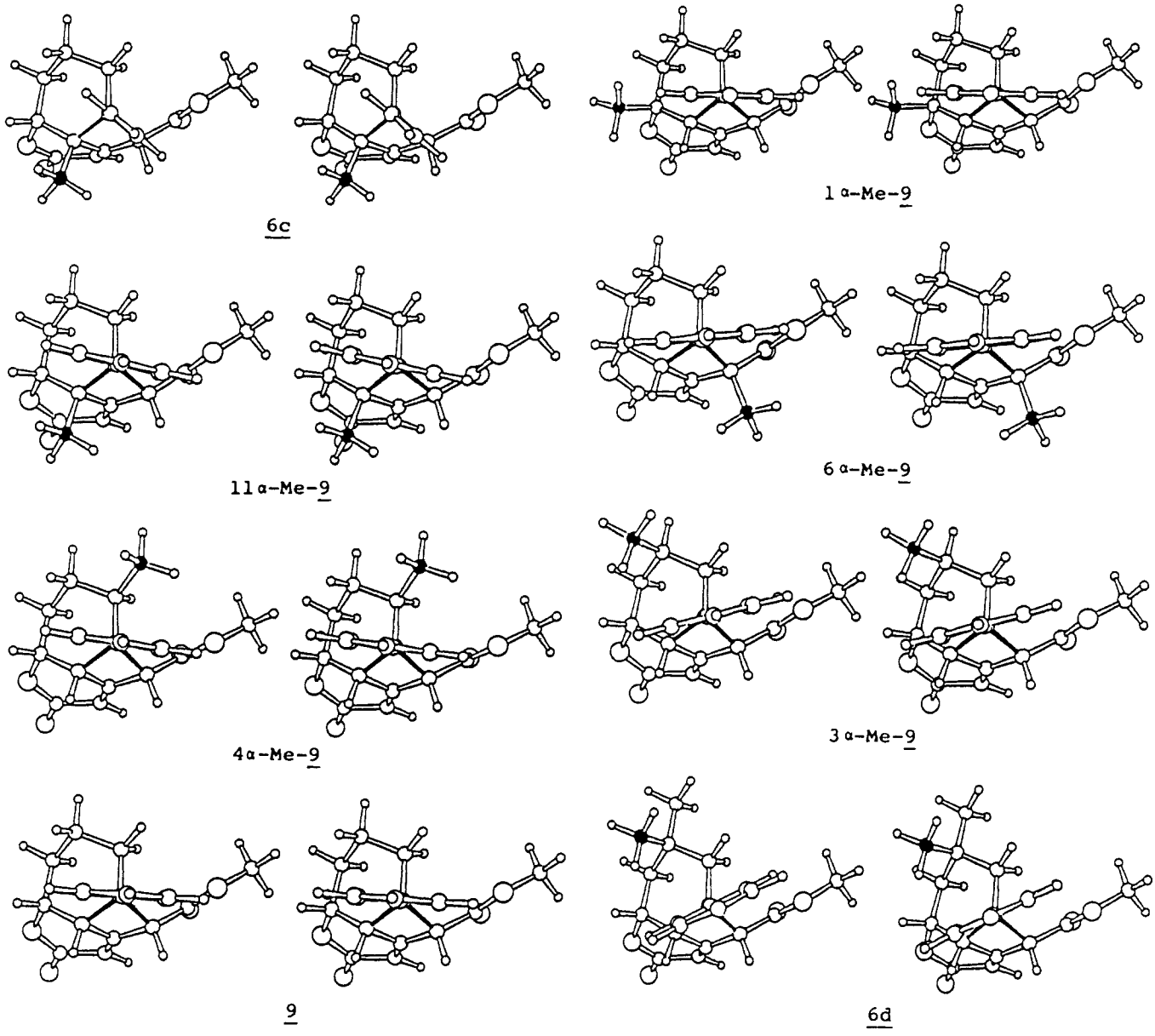

Figure 4. ORTEP stereoprojections of **6c**, **6d**, and **9** as viewed down from the phenyl group along its bond to C_5. **6c** and **6d** are drawn on the basis of the X-ray coordinates, whereas each structure of **9** represents the lowest energy conformer with regard to the rotation of the C_5–phenyl bond.

5.09 (d, 1 H, J = 10.8 Hz), 5.22 (d, 1 H, J = 16.8 Hz), 5.50 (m, 1 H), 5.67 (m, 1 H), 6.02 (s, 2 H), 6.42 (dd, 1 H, J = 10.8, 16.8 Hz).

Methyl 3-vinyl-2-cyclohexenyl penta-2,3-diene-1,5-dioate (5b): pale yellow oil in 70% yield; IR (neat) 1960, 1720 cm^{-1}; ^1H NMR ($CDCl_3$) δ 1.57–1.86 (m, 4 H), 2.05–2.18 (m, 2 H), 3.78 (s, 3 H), 5.08 (d, 1 H, J = 10.2 Hz), 5.25 (d, 1 H, J = 17.4 Hz), 5.5 (m, 1 H), 5.72 (m, 1 H), 6.04 (s, 2 H), 6.38 (dd, 1 H, J = 10.2, 17.4 Hz).

Methyl 2-methyl-3-vinyl-2-cyclohexenyl penta-2,3-diene-1,5-dioate (5c): pale yellow oil in 71% yield; IR (neat) 1960, 1725 cm^{-1}; ^1H NMR ($CDCl_3$) δ 1.64–2.20 (m, 4 H), 1.78 (s, 3 H), 3.77 (s, 3 H), 5.13 (d, 1 H, J = 10.8 Hz), 5.27 (d, 1 H, J = 17.4 Hz), 5.4 (m, 1 H), 6.04 (br s, 2 H), 6.80 (dd, 1 H, J = 10.8, 17.4 Hz).

Methyl 3-phenyl-5,5-dimethyl-2-cyclohexenyl penta-2,3-diene-1,5-dioate (5d): pale yellow oil in 84% yield; IR (neat) 1960, 1720 cm^{-1}; ^1H NMR ($CDCl_3$) δ 0.95–2.30 (m, 4 H), 1.04 (s, 3 H), 1.09 (s, 3 H), 3.77 (s, 3 H), 5.63 (m, 1 H), 6.04 (s, 2 H), 7.24–7.35 (m, 6 H).

(9a*SR*,9b*RS*)-2,4,5,7,8,9,9a,9b-Octahydro-2-oxo-4-(methoxycarbonyl)-8,8-dimethylnaphtho[1,8-*bc*]pyran (6a). A solution of the allene-1,3-dicarboxylate **5a** (282 mg, 1.02 mmol) in dry *o*-xylene (200 mL) under argon was heated to reflux for 2 h. The reaction mixture was rotary evaporated, and the residue was chromatographed on silica gel with *n*-hexane–ethyl acetate (4:1) as eluent to afford the [4 + 2] cycloadduct **6a** (268 mg, 95%) as yellow oil. Spectral data are summarized in Table II.

(9a*SR*,9b*RS*)-2,4,5,7,8,9,9a,9b-Octahydro-2-oxo-4-(methoxycarbonyl)naphtho[1,8-*bc*]pyran (6b). In the same manner as described above, the allene-1,3-dicarbxoylate **4b** (300 mg, 1.21 mmol) afforded the [4 + 2] cycloadduct **6b** (207.3 mg) as colorless needles in 69% yield. ^{13}C NMR ($CDCl_3$): δ 19.4, 29.7, 31.9, 33.7, 40.9, 47.4, 52.4, 73.5, 112.4, 120.9, 135.4, 158.9, 164.9, 170.7. Anal. Calcd for $C_{14}H_{16}O_4$: C, 67.72; H, 6.50. Found: C, 67.65; H, 6.50.

2,3,7,8,9,9a-Hexahydro-2-oxo-4-(methoxycarbonyl)-8,8-dimethylnaphtho[1,8-*bc*]pyran (7a). A solution of **6a** (111 mg, 0.4 mmol) and 5% Pd–C (58 mg) in dry *o*-xylene (10 mL) was heated to reflux for 4 h. The Pd–C catalyst was filtered off and washed with dry benzene. The filtrate and washings were combined, and the solution was rotary evaporated. The residue was crystallized from diethyl ether–*n*-hexane (1:1) as colorless crystals **7a** (87.4 mg, 79.4%). ^{13}C NMR ($CDCl_3$): δ 25.3, 31.1, 31.6, 34.7, 40.8, 42.8, 52.2, 73.9, 125.9, 127.7, 130.9, 131.1, 133.6, 140.2, 166.8, 171.1. Anal. Calcd for $C_{16}H_{18}O_4$: C, 70.06; H, 6.61. Found: C, 69.98; H, 6.61.

2,3,7,8,9,9a-Hexahydro-2-oxo-4-(methoxycarbonyl)naphtho[1,8-*bc*]-pyran (7b). In the same manner as described above, **6b** (100 mg, 0.404 mmol) afforded the aromatized compound **7b** (34.6 mg, 0.141 mmol) as colorless needles in 34.9% yield (quantitative yield based on recovery of **5b**). Anal. Calcd for $C_{14}H_{14}O_4$: C, 68.28; H, 5.73. Found: C, 68.12; H, 5.73.

(1*RS*,5*RS*,6*RS*,11*SR*)-5-Vinyl-6-(methoxycarbonyl)-11-methyl-10-oxatricyclo[5.3.1.$0^{5,11}$]undec-7(8)-en-9-one (6c). In the same manner, the thermal treatment of **5c** (297.9 mg, 1.14 mmol) afforded the [2 + 2] cycloadduct **6c** (94.4 mg, 0.36 mmol) as colorless needles (from isopropyl ether) in 31.6% yield. ^{13}C NMR ($CDCl_3$): δ 19.4, 20.7, 29.4, 31.4, 42.9, 51.1, 52.0, 52.4, 82.2, 111.3, 114.9, 138.5, 157.7, 162.6, 168.8. Anal. Calcd for $C_{15}H_{18}O_4$: C, 68.69; H, 6.92. Found: C, 68.84; H, 6.94.

Several recrystallizations afforded a pure enantiomer of **6c**: $[\alpha]^{25}_D$ -18.7° (*c* 0.076, $CHCl_3$); mp 158-160 °C. This enantiomer gave one doublet for the olefinic proton in the presence of 0.2 equiv of chiral shift reagent tris[3-[(heptafluoropropyl)hydroxymethylene]-*d*-camphorato-[europium(III) [Eu(hfc)] at 270 MHz. This spectrum indicated an ee >99%. In contrast, a similar solution of racemic mixture of **6c**, as resulting from the first recrystallization of reaction product, gave two doublets ($\Delta\nu$ = 2.14 Hz) for the olefinic proton. On the other hand, the filtrate of that recrystallization was evaporated and recrystallized to afford an antipode, $[\alpha]^{24}_D$ +14.9° (*c* 0.388, $CHCl_3$).

(1*RS*,5*RS*,6*RS*,11*SR*)-5-Phenyl-6-(methoxycarbonyl)-3,3-dimethyl-10-oxatricyclo[5.3.1.0^{5,11}]undec-7(8)-en-9-one (6d). In the same manner, the thermal treatment of **5d** (502.6 mg, 1.54 mmol) afforded the [2 + 2] cycloadduct **6d** (205.5 mg, 0.63 mmol) as colorless needles in 40.9% yield. ^{13}C NMR ($CDCl_3$): δ 23.4, 32.4, 32.8, 38.0, 39.7, 45.0, 50.0, 52.3, 60.4, 75.0, 111.9, 126.1, 126.8, 128.6, 147.0, 152.7, 162.6, 168.3. Anal. Calcd for $C_{20}H_{22}O_4$: C, 73.60; H, 6.79. Found: C, 73.64; H, 6.80.

X-ray Crystallography. Crystal Data. $C_{15}H_{18}O_4$ (**6c**), M_r 262.31: monoclinic; $P2_1$; a = 12.583 (1), b = 7.620 (1), c = 7.318 (1) Å; V = 679.2 Å^3; D(calcd) = 1.282 g cm^{-3}; Z = 2; λ(Cu Kα) = 1.5418 Å; μ = 7.2 cm^{-1}; F(000) = 280. Colorless prisms of **6c** grew from diisopropyl ether by slow evaporation at room temperature. The crystal, with dimensions of 0.10 × 0.20 × 0.20 mm, was employed for the experiments on Enraf-Nonius CAD4 diffractometer with graphite monochromator. Lattice parameters were determined on 25 2θ values (22° <2θ < 64°) by the least-squares procedure. Intensity data were collected by θ-2θ scans to a limit of 2θ = 150°, with scan rate 1.65-4.12° min^{-1} in θ and with scan width (0.45 + 0.14 tan θ)°. Range of indices inclusive are $-15 \le h \le 15$, $0 \le k \le 9$, $0 \le l \le 9$. Three standard reflections were monitored after every measurement of 200 reflections for the check of orientation and at the interval of 2 h for the check of intensity. The variation of standards was less than 0.6% of the 1511 independent reflections; 1420 were treated as observed ($|F_o| > 2\sigma|F_o|$). Systematic absences were 0*k*0, *k* odd. The intensities were corrected for Lorentz and polarization effects, but no correction was applied for absorption. $C_{20}H_{22}O_4$ (**6d**), M_r 326.40: monoclinic; $P2_1/a$; a = 16.311 (1), b = 9.959 (1), c = 10.605 (1) Å; β = 95.15 (1)°; V = 1715.9 Å^3; D(calcd) = 1.263 g cm^{-3}; Z = 4; λ(Cu Kα) = 1.5418 Å; μ = 6.7 cm^{-1}; F(000) = 696. Colorless prisms of **6d** grew from diisopropyl ether: crystal size 0.18 × 0.43 × 0.43 mm; Enraf-Nonius CAD4 diffractometer; θ-2θ scan; 1.27-4.12° min^{-1} in θ; scan width (0.45 + 0.14 tan θ)°; range of indices $-20 \le h \le 20$, $0 \le k \le 12$, $0 \le l \le 13$ (2θ < 150°). Lattice parameters were determined on the basis of 25 2θ values (46° < 2θ < 140°). Variation of standard was <0.3%; 3760 reflections were measured; 3060 reflections were observed with $|F_o| > 2\sigma(|F_o|)$. Systematic absences *h*0*l*, *h* odd, 0*k*0, *k* odd. No corrections for absorption were made.

Structure Determination. Crystal structure was solved by direct methods with the program MULTAN/82[13] and refined by full-matrix least-squares method. All hydrogen atoms were refined by full-matrix least-squares method. All hydrogen atoms were located by stereochemical calculation. Non-hydrogen atoms were refined with anisotropic thermal parameters, and hydrogen atoms, with isotropic thermal parameters (B = 5.0, fixed). $\sum w(|F_o| - |F_c|)^2$ was minimized. The weighting scheme for **6c** was as follows: w = 1.0 for F_o < 721.7, $w = (721.7/F_o)^2$ for $F_o \ge 721.7$. Final R index was 0.033, and R_w was 0.030. Secondary extinction factor (g) was refined: 1.18 (2) × 10^{-5} [$|F_o| = |F_c|/(1 + glc)$]. Δ/σ was less than 1.2, and the largest peak in the final difference Fourier map was +0.14 e Å^{-3}. The absolute configuration of the molecule (6*R*,13*R*,17*R*,18*S*) was determined by the Bijvoet method, taking into account the anomalous dispersion effect of oxygen atom for Cu Kα radiation. The same procedure was applied for **6d**. Weighting scheme: w = 1.0 for F_o < 1484.3, $w = (1484.3/F_o)^2$ for $F_o \ge 1484.3$. Final R = 0.048, and R_w = 0.044. Secondary extinction factor (g) was 4.27 (4) × 10^{-6}. Δ/σ < 1.1, and the largest peak in the final ΔF map was +0.20 e Å^{-3}. Atomic scattering factors were taken from ref 16. All the calculations were performed on a DEC VAX 11/730 computer with the programs of Enraf-Nonius SDP[14] and ORTEP II.[15]

Method of Molecular Orbital (MO) and Empirical Force-Field Calculations. QCPE Program MMP2[9] was used for molecular mechanics calculations. Calculations were carried out at the Computing Centers of Hokkaido University and the Institute for Molecular Science.

Supplementary Material Available: Tables of thermal parameters and torsional angles for **6c** and **6d** (5 pages); tables of observed and calculated structure factors (23 pages). Ordering information is given on any current masthead page.

(13) Main, P.; Fiske, S. J.; Hull, S. E.; Lessinaer, L.; Germain, G.; Declerq, J.-P.; Woolfson, M. M. *A System of Computer Programs for the Automatic Solution of Crystal Structures from X-ray Diffraction Data*; University of York: England, 1982.

(14) Frenz, B. A. *Structure Determination Package*; College Station, TX, and Enraf-Nonius, Delft, The Netherlands, 1984.

(15) Johnson, C. K. ORTEP II, Report ORNL-5138; Oak Ridge National Laboratory: Oak Ridge, TN, 1976.

(16) *International Tables for X-ray Crystallography*; Kynoch: Birmingham, England, 1974.

Asymmetric Diels-Alder Cycloaddition Reactions with Chiral α,β-Unsaturated *N*-Acyloxazolidinones

D. A. Evans,* K. T. Chapman, and J. Bisaha

Contribution from the Department of Chemistry, Harvard University, Cambridge, Massachusetts 02138. *Received June 22, 1987*

Abstract: Chiral α,β-unsaturated *N*-acyloxazolidinones are highly reactive and highly diastereoselective dienophiles in Diels-Alder reactions promoted by dialkylaluminum chlorides. A cationic Lewis acid-dienophile complex is proposed to account for the observed exceptional reactivity and endo/exo selectivities. Acrylate and (*E*)-crotonate carboximides bearing phenylalaninol-derived oxazolidinones undergo rapid and selective cycloadditions with the relatively unreactive dienes isoprene and piperylene at temperatures as low as -100 °C. Intramolecular cycloadditions of (*E*,*E*)-2,7,9-decatrienimides and (*E*,*E*)-2,8,10-undecatrienimides proceed with high diastereoface selectivity and virtually complete endo/exo selectivity. In all cases, high yields of diastereomerically homogeneous products may be obtained by simple recrystallization or silica gel chromatography. Nondestructive chiral auxiliary removal is facile with even the most sterically hindered Diels-Alder adducts. The enhanced diastereoselectivities observed in Diels-Alder reactions of phenylalaninol-derived dienophiles are shown not to be steric in origin but a result of electronic interactions involving the phenyl ring. The technique employed to expose this electronic effect, comparison of diastereoselectivities in analogous alkylation and Diels-Alder reactions, directly provides transition-state structural information.

The venerable Diels-Alder reaction has provided fertile ground for asymmetric reaction engineering. Several recent reviews describe impressive progress in this area, which has included the design of chiral dienophiles, dienes, and Lewis acid catalysts.[1]

0002-7863/88/1510-1238$01.50/0